AJNR

Stent-Assisted Coiling of Intracranial Aneurysms Aided by Virtual Parent Artery Reconstruction

Christof Karmonik, Charles M. Strother, Xiaoyan Chen, Frank Deinzer, Richard Klucznik and Michel E. Mawad

AJNR Am J Neuroradiol 2005, 26 (9) 2368-2370
http://www.ajnr.org/content/26/9/2368

AJNR Am J Neuroradiol 26:2368–2370, October 2005

Technical Note

Stent-Assisted Coiling of Intracranial Aneurysms Aided by Virtual Parent Artery Reconstruction

Christof Karmonik, Charles M. Strother, Xiaoyan Chen, Frank Deinzer, Richard Klucznik, and Michel E. Mawad

Summary: The availability of stents designed specifically for use in the intracranial vasculature has increased the use of stent-assisted coiling for treatment of wide-necked and complex intracranial aneurysms. We present a technique for pretreatment planning and visualization of a virtual stent within the parent artery by using a virtual reconstruction of the parent artery across the aneurysm neck. As illustrated by 2 clinical examples, this method provides information not otherwise available regarding the location of portions of the stent that are not visible on fluoroscopy. During treatment, this information enhances the ability to determine the location of coils in relation to the stent boundaries and should thereby improve the ability to avoid parent artery compromise.

As a result of the complex relations between many aneurysms and their parent artery and the inability to visualize a stent fluoroscopically, it is often difficult to achieve a working projection adequate to ensure that loops of coils are confined behind a stent and are not compromising the parent artery lumen. Consequently, we often find it necessary to use balloon-neck protection as an adjunct to stent-assisted coiling. Because this adds complexity to the procedure, we have developed and retrospectively evaluated a pretreatment postprocessing algorithm that provides a virtual image of the full extent of a stent in the parent artery. Use of this technique seems likely to then facilitate the ability to understand, during treatment, the location of coils as they are placed and detached into an aneurysm.

Description of the Technique

Angiographic data were obtained with a bi-plane C-arm system (Axiom Artis, Siemens Medical System, Erlangen, Germany) by using commercially available hardware and software. The algorithm used for creating a virtual image of the full extent of a stent in the parent artery was implemented as a plug-in for the 3D image postprocessing software package, InSpace, on the Siemens Leonardo workstation (version 2004B) as a research prototype. The technical details of this algorithm are considered confidential intellectual property at this time. A patent is pending. All images were analyzed retrospectively after treatment had been completed.

After a volume of interest containing the aneurysm and proximal and distal segments of the healthy parent artery had been chosen by manually clipping the 3D digital subtraction angiogram (3D-DSA) data, the centerline of the normal segments of the parent artery proximal and distal to the aneurysm was computed by using a skeletonization algorithm. From these centerline segments, the centerline of the parent artery across the aneurysm ostium was then interpolated. With this interpolation approach, an application of the presented technique to the most general case of a fusiform aneurysm within a curved vessel segment is possible. The quality of the reconstructed artery segment will depend on the particular details of the curvature and how well it can be interpolated from the healthy vessel segments adjacent to the aneurysm. Visual inspection of the results will always be necessary to verify a satisfying performance of the algorithm.

Next, a set of contiguous 2D cross-sections (cut planes) (~0.1-mm thickness) that contained the entire volume of the normal parent artery segments and the aneurysm and that was oriented perpendicular to the interpolated centerline was obtained. Then, for each cross-section containing a portion of the aneurysm, the corresponding radius of the virtual parent artery was linearly interpolated by using the radii measured at the normal proximal and distal segments of the parent artery. In this way, any natural tapering of the parent artery, if visible in the original 3D-DSA images, was taken into account by the algorithm.

The resulting reconstruction was then projected for analysis in 3 different views: (1) as a series of 2D cross-sections; (2) as a 3D cut surface reconstruction (clipped by a cut plane to allow inspection of the inside of the aneurysm); and (3) as a 3D surface-rendered volume.

Using this technique, we assessed the morphology of 2 aneurysms that were treated with stent-assisted

Received January 31, 2005; accepted after revision May 12.

From the Department of Radiology, Baylor College of Medicine (C.K., C.M.S., M.E.M.), Houston, TX; the Department of Radiology, The Methodist Hospital (R.K., M.E.M.), Houston, TX; and Siemens Medical Systems (X.C., F.D.), Erlangen, Germany.

Address correspondence to Christof Karmonik, PhD, Department of Radiology, The Methodist Hospital, M 214, 6565 Fannin, Houston, TX 77030

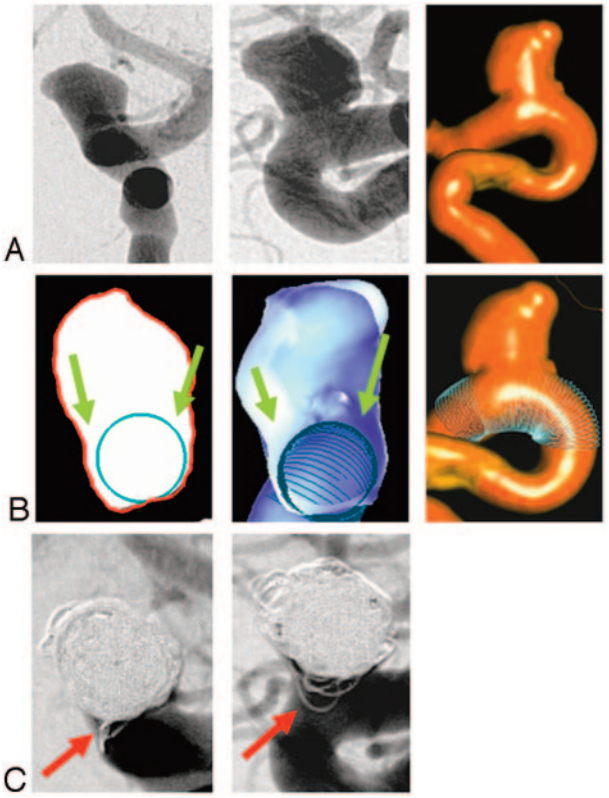

FIG 1. (*A*) 2D-DSA pretreatment projection images (*left*: AP view, *center*: lateral view) and 3D-DSA surface volume reconstruction (*right*) for case 1. (*B*) Virtual artery reconstruction (*left*: selected cut-plane section; *center*: cut-surface volume reconstruction; *right*: 3D-DSA surface volume reconstruction). The blue circles mark the location of the virtual artery in each picture. The green arrows depict "pockets" or cul-de-sacs around the virtually reconstructed artery. (*C*) 2D-DSA posttreatment projection images (*left*: AP view; *right*: lateral view). Coil loops in the "pocket" along the medial side of the aneurysm appear to lie within the parent artery. Comparison with the cut-plane section and the cut-surface reconstruction in (*B*); however, show that they are actually located outside the stent.

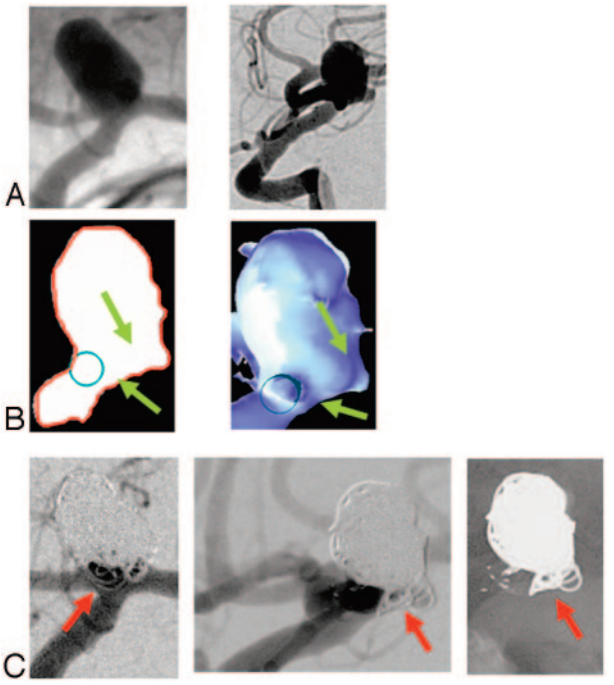

FIG 2. (*A*) 2D-DSA pretreatment projection images (*left*: AP view; *right*: lateral view) for case 2. (*B*) Virtual artery reconstruction (*left*: selected cut-plane section; *right*: cut-surface volume reconstruction). The blue circles mark the position of the virtual artery. The green arrows demonstrate the extension of the aneurysm ostium posterior to the boundary of the parent artery. (*C*) 2D posttreatment projection images (*left*: DSA AP view; *center*: DSA lateral view; *right*: native lateral view). Red arrows depict coils that appear to be within the parent artery.

coiling. One was a paraophthalmic aneurysm having a sidewall geometry (case 1) and the other was a carotid bifurcation aneurysm (case 2).

Case 1: Wide-Neck Paraophthalmic Aneurysm

The pretreatment anteroposterior (AP) and lateral 2D-DSA projection images clearly show the course and size of the parent artery, the aneurysm size, and the neck length (Fig 1*A*, *left* and *center*). The 3D-DSA surface volume reconstruction shows to better advantage the expansion and irregularity of the portion of the ventral wall of the internal carotid artery from which the aneurysm arises (Fig 1*A*, *right*). Neither of these show, however, that the aneurysm ostium involves at least 180 degrees of the parent artery circumference. This feature is clearly shown in the cut-plane section and the cut-surface volume reconstruction (Fig 1*B*, *left* and *center*). Both of these also demonstrate well the "pockets" of the aneurysm that lie outside of the boundaries of the virtual stent. The fit of the virtual stent can be verified in the 3D-DSA surface volume reconstruction (Fig 1*B*, *right*). Coil loops in the "pocket" along the medial side of the aneurysm appear to lie within the parent artery on the AP and lateral 2D-DSA projection images (Fig 1*C*). During treatment it was not possible to achieve a working projection that separated clearly this component of the aneurysm from the parent artery.

Case 2: Wide-Neck Carotid Bifurcation Aneurysm

The AP and lateral pretreatment 2D-DSA projection images show clearly the course of the parent artery, the aneurysm size and the neck length. (Fig 2*A*). The cut-plane section and cut-surface volume reconstruction in a lateral projection and with a circle inserted to show the location and size of the interpolated normal parent artery demonstrate the extension of the aneurysm ostium posterior to the boundary of the parent artery (Fig 2*B*). Posttreatment AP and lateral subtracted and unsubtracted images show coils that appear to be within the parent artery (Fig 2*C*). Comparing these with the cut-plane section and cut-surface volume reconstruction shows that these are, in fact, outside of the boundaries of the stent and are not compromising the parent artery.

Discussion

The availability of stents designed for use in the endovascular treatment of aneurysms has enhanced the ability to treat wide-neck intracranial aneurysms with endovascular techniques (1, 2). In our experience, because of the inability to directly visualize these stents fluoroscopically, it is often difficult, or impossible, to achieve a working projection adequate to be sure that coils or coil loops are not herniating through a stent cell and causing parent artery compromise. Because of this, we commonly employ balloon-neck protection in conjunction with stent-assisted coiling. As this increases the complexity, and possibly the risks of the procedure, we have developed a technique that allows full visualization of a virtual stent deployed across an aneurysm ostium. If the technique were available as a pretreatment planning aid, this would seem to offer enhanced ability to visualize and to understand the complex relations between an aneurysm and its parent artery.

Although commercially available 3D-DSA postprocessing techniques allow the depiction of the external anatomical features of intracranial aneurysms, they fail to depict clearly the topography of an aneurysm ostium to its parent artery. In an earlier publication we described and illustrated a technique for using 3D-DSA datasets to better characterize aneurysm morphology (3). In this report, we describe an extension of that technique that allows insertion and visualization of a virtual stent.

Using conventional image intensifier angiographic systems and a variety of postprocessing techniques, we have not been able to adequately visualize stents made of nitinol. We have, however, recently acquired a flat detector angiographic system, and early experience with this system indicates that it greatly enhances our ability to visualize these devices. Thus far, none of these techniques provide visualization equal to that obtained with the virtual stent technique.

The 2 examples given illustrate how the ability to visualize a virtual stent before treatment should improve the ability to monitor coil deposition during treatment because it provides the operator with a priori knowledge—both about the aneurysm ostium and about the parent artery and the location of stent boundaries that cannot be visualized directly during treatment.

Our technique does not model the stent deployment by highly sophisticated means such as finite elements, but rather assumes that a stent deployed so that it passes from a proximal segment of normal artery, across an aneurysm ostium, and into a distal segment of parent artery, will reconstruct the arterial boundaries to duplicate those of a normal artery. Looking at the 3D-DSA volume reconstructions for the 2 examples shown, one can see that the excellent fit of the reconstructed artery from which the aneurysm arises with the normal proximal and distal segments indicates that, in these 2 examples, this assumption is valid.

Conclusion

The technique described allows visualization of a virtual stent in 3D-DSA volume reconstructions. This provides information that will be valuable in pretreatment planning and should also facilitate verification that coils are not herniating through nonvisible portions of stents used for stent-assisted coiling.

References

1. Alfke K, Straube T, Dorner L, Mehdorn HM, Jansen O. **Treatment of intracranial broad-neck aneurysms with a new self-expanding stent and coil embolization.** *AJNR Am J Neuroradiol* 2004;25:584–591
2. Wanke I, Doerfler A, Schoch B, Stolke D, Forsting M. **Treatment of wide-necked intracranial aneurysms with a self-expanding stent system: Initial clinical experience.** *AJNR Am J Neuroradiol* 2003;24:1192–1199
3. Karmonik C, Arat A, Benndorf G, et al. **A Technique for improved quantitative characterization of intracranial aneurysms.** *AJNR Am J Neuroradiol* 2004;25:1158–1161